

A Inductor Average Current Mode Controller Plus Proportional Integral Controller for a Bi-Directional AC-DC Power Converter with Power Factor Correction for DC Micro Grid

¹ J. R. Abilash, ²Dr. A. Amudha², Dr. M. Siva Ramkumar³ Dr. G. Emayavaramban⁴, Dr. Viyathukattuva⁵, P. Nagaveni⁶,

¹Dept of EEE, Faculty of Engineering, Karpagam Academy of Higher Education, Coimbatore,
^{3,4,5,6}Asst Prof, Dept of EEE, Faculty of Engineering, Karpagam Academy of Higher Education, Coimbatore,
²Prof & Head, Dept of EEE, Faculty of Engineering, Karpagam Academy of Higher Education, Coimbatore
amudha.a@kahedu.edu.in

Article Info

Volume 83

Page Number: 2529 - 2544

Publication Issue:

March - April 2020

Abstract:

This paper presents the current mode controller for two-directional ac-dc power converter with power factor correction for dc micro grid. The performance of the designed model is justified with help of MATLAB/Simulink software. The results are presented to show the proficient of the developed model.

Article History

Article Received: 24 July 2019

Revised: 12 September 2019

Accepted: 15 February 2020

Publication: 19 March 2020

1. Introduction

In current scenario, the power factor correction converters are plays a major role in many applications. Most of the power converters fed non-linear load draws the non-disturbed input current waveform from the mains. The conventional methods of AC-DC power with filter has major problems [1-8]. The current controllers for various power factor correction converters have been reported [9-13]. Therefore, in this paper, it is propose a SCR based AC-DC bidirectional power converter with proficient power factor. The main benefits of this designed model has minimal cost, small capacitor size, good power factor and output voltage regulation.

1. Operation of Bi-Directional AC-DC Power Converter

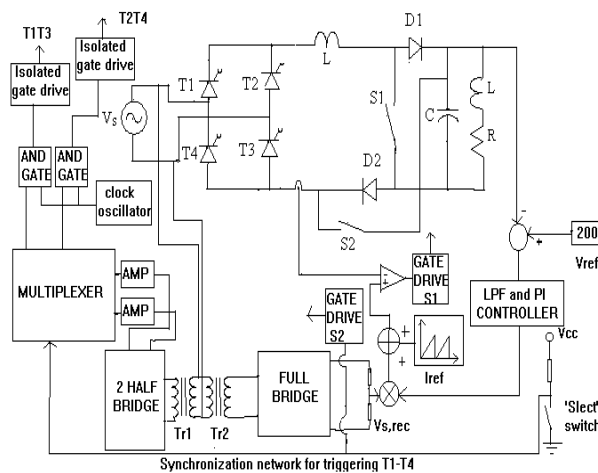


Fig.1 Proposed bidirectional ac-dc power converter

Fig.1 shows the ac-dc bi-directional converter. It consists of power circuit and inductor average current controller and the synchronization circuit for triggering the thyristor. Power conversion stage consists of four low cost, SCRs T1-T4, switches (S1 & S2), D1 & D2, L and C.

2.1 Motoring mode operation

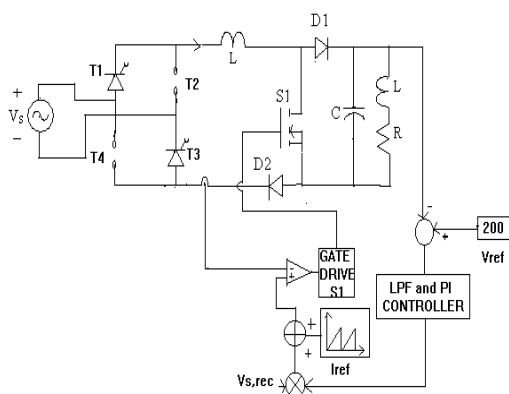


Fig.2 Motoring mode operation during positive half cycle of supply

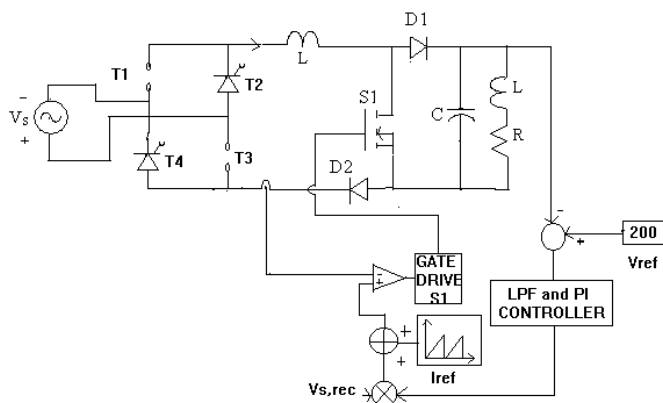


Fig.3 Motoring mode operation during negative half cycle of supply

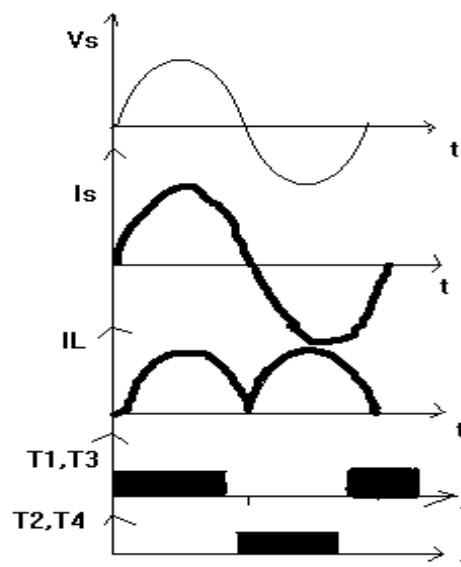


Fig.4 Timing diagram

The firing of T1-T4 are synchronized with the supply voltage in fig.1 and its switching diagram in figs 2,3, and 4. In motoring mode, T1 and T3 are turned on at an angle 345° in the positive half cycle of supply voltage whereas T2 and T4 are turned on at an angle 165° that gives an input voltage for the chopper circuit, similar to that of a diode rectifier. S2 is open for the whole motoring mode. As in fig.11 the feedback current i_{fb} is compared with the reference sinusoidal waveform i_{ref} and is forced to remain between the maximum and the minimum values of i_{ref} . Topology AI-fig.4(a): i_L is defined as

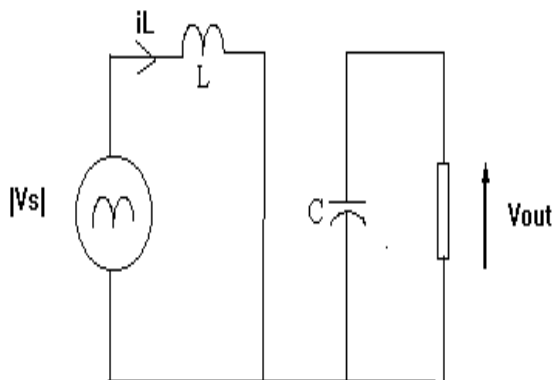


Fig. 4(a) Operation boost converter-I

$$i_L(t) = i_{L,0} + \frac{V_S}{L}t \quad (1)$$

$i_{L,0}$ is the initial value of i_L at the beginning of a switching cycle. At the end of this interval dT_s

$$i_{L,dT_s} = i_{L,0} + \frac{V_S d T_s}{L} \quad (2)$$

➤ Topology AII-fig.4(b)&(c):

➤

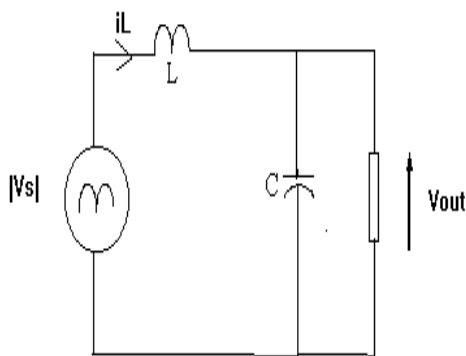


Fig. 4(b) Operation of boost converter-II

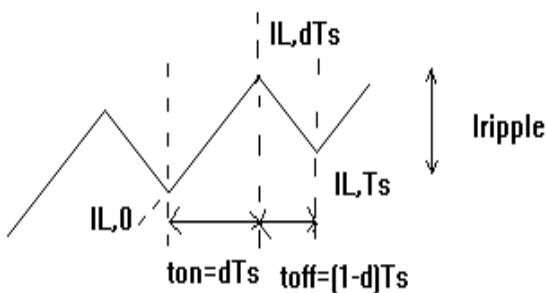


Fig. 4(c) Inductor current

$$i_L(t) = i_{L,dT_s} + \frac{V_S - V_{out}}{L}t$$

$$i_L(t) = i_{L,0} + \frac{V_S d T_s}{L} + \frac{V_S - V_{out}}{L}t \quad (3)$$

At the end of the half cycle

$$i_{L,Ts} = i_{L,0} + \frac{V_S T_s}{L} - \frac{V_{out}}{L}(1-d)T_s \quad (4)$$

By using equation (4), the ideal quasi steady state conversion characteristics is given by

$$|V_S| = V_{out} (1-d) \quad (5)$$

$$\text{As, } |V_S| = V_m |\text{Sin}\omega t|$$

$$d(t) = 1 - \frac{V_m}{V_{out}} |\text{Sin}\omega t| = 1 - \frac{1}{M_1} |\text{Sin}\omega t| \quad (6)$$

(6)

Where

$$M_1 = V_{out}/V_m$$

2.2 Regenerating mode operation

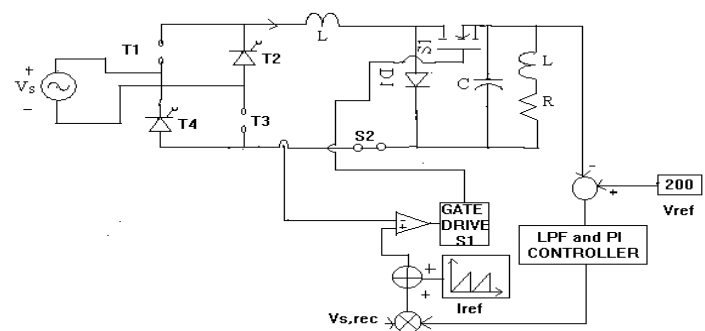


Fig.5 Regenerating mode + ve half cycle of power source

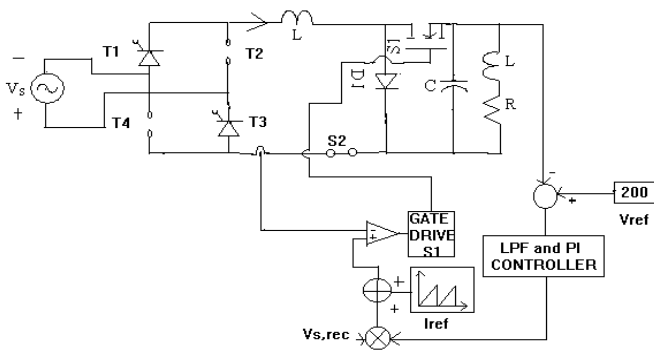


Fig.6 Regenerating mode - ve half cycle of power source

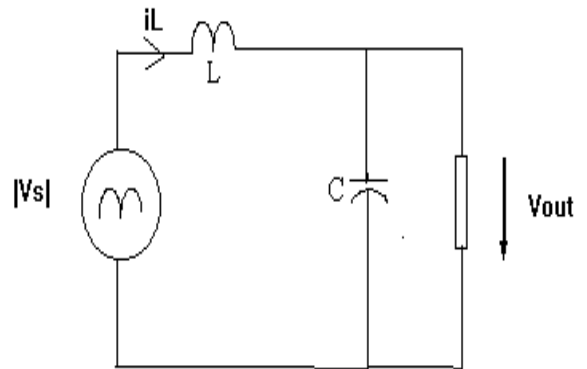


Fig.7(a) Operation of buck converter-I

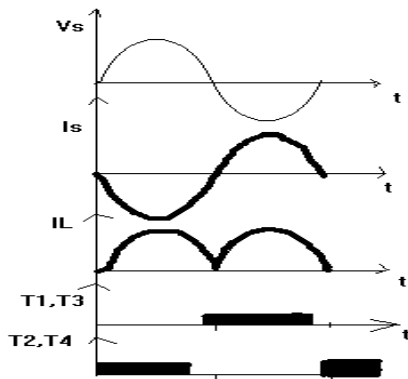


Fig.7 Timing diagram

During the regenerating mode S2 is turned on and D2 is reverse biased. In this mode T1-T4 are operated in anti-phase with the operation in motoring mode, which gives the reverse input voltage. The converter now acts as a buck converter with voltage across the bulk capacitor as the input voltage. In regenerating mode when the switch S1 is closed the inductor current will rise and the current will flow from the load to supply through the thyristor. Fig.7(a): In one switching cycle, i_L is given by

$$i_L(t) = i_{L,0} + \frac{V_{out} - V_s}{L} t$$

(7)

$i_{L,0}$ is the initial value of i_L at the beginning of a switching cycle. This stage is defined by the ON time of S1 (dT_s). At the end of this stage

$$i_{L,dT_s} = i_{L,0} + \frac{V_{out} - V_s}{L} dT_s$$

(8)

➤ Topology BII-fig.7(b)&(c): i_L is given by

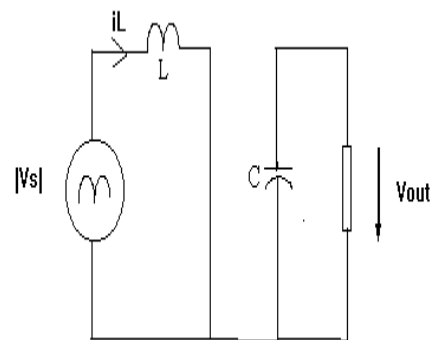


Fig.7(b) Operation of buck converter-II

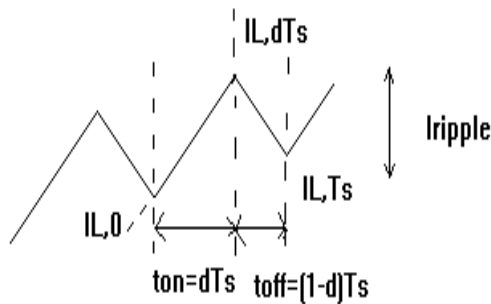


Fig. 7(c) Inductor current

$$i_L(t) = i_{L,dTs} - \frac{V_s}{L}t$$

(9)

This stage is defined for period of $T_{off} = (1-d) T_s$.
Therefore

$$i_{L,Ts} = i_{L,0} - \frac{V_{out} - V_s}{L} dT_s - \frac{V_s}{L} (1-d)T_s$$

(10)

By using equation (10), the ideal quasi steady state conversion characteristics is given by

$$|V_s| = d V_{out}$$

(11)

$$\text{As } |V_s| = V_m |\sin \omega t|,$$

$$d = \frac{V_m}{V_{out}} |\sin \omega t| = \frac{1}{M2} |\sin \omega t|$$

(12)

Where

$$M2 = V_{out} / V_m$$

2.3 Average output current

Motoring mode: If the input current of the converter is assumed to be perfectly sinusoidal and the conversion efficiency is assumed to be 100%

$$i_s = i_m |\sin \omega t|$$

$$\frac{1}{\pi} \int_0^\pi V_s i_s d\omega t = i^2_{out,avg} R_L$$

$$\frac{1}{2} V_m I_m = i^2_{out,avg} R_L$$

$$i_{out,avg} = \sqrt{I_m V_m / 2} R_L \quad (13)$$

Where

I_m is the peak value of supply current

As I_m is controlled by the current controller, the output voltage can be varied by changing the I_{ref} .

Regenerative mode: Again if supply current is assumed to be sinusoidal and conversion efficiency is 100%

$$i_s = -i_m |\sin \omega t|$$

$$\frac{1}{\pi} \int_0^\pi V_s i_s d\omega t = -i_{out,avg} V_{out}$$

$$\frac{1}{2} V_m I_m = i_{out,avg} V_{out}$$

$$i_{out,avg} = \frac{I_m}{2M2}$$

(14)

2.4 Design the value of inductance (L)

Motoring mode: Considering the input current in fig.8 it's peak to peak value I_{ripple} is given as

$$i_{\text{ripple}} = \frac{V_s d T_s}{L} = \frac{V_m T_s}{L} \left| \sin \omega t \right| \left(1 - \frac{1}{M1} \left| \sin \omega t \right| \right) \quad (15)$$

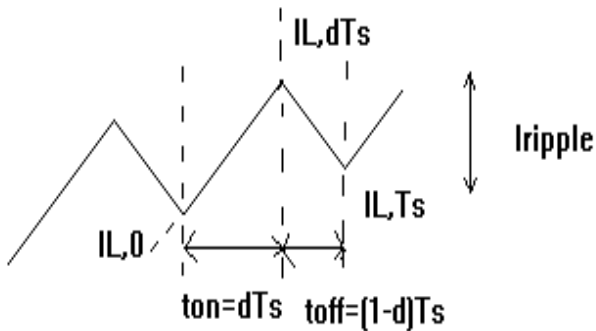


Fig. 8 Inductor current

Differentiating i_{ripple} with respect to $\sin \omega t$ and equating the expression to zero gives

$$1 - \frac{2}{M2} \left| \sin \omega t \right| = 0 \quad (16)$$

$$i_{\text{ripple}} = \frac{V_m M1 T_s}{4 L_{\text{min}}} \quad (18)$$

$$L_{\text{min}} = V_m M1 T_s / 4 i_{\text{ripple}}$$

Regenerative mode: As in fig.8 the ripple current flowing through the inductor is

$$i_{\text{ripple}} = \frac{(V_{\text{out}} - V_s)}{L} d T_s$$

$$\begin{aligned} &= \frac{(V_{\text{out}} - V_m \left| \sin \omega t \right|) d \left| \sin \omega t \right| T_s}{L} \\ &= \frac{V_{\text{out}} T_s}{L} \left(1 - \frac{1}{M2} \left| \sin \omega t \right| \right) \frac{1}{M2} \left| \sin \omega t \right| \\ &= \frac{V_m T_s}{L} \left| \sin \omega t \right| \left(1 - \frac{1}{M2} \left| \sin \omega t \right| \right) \end{aligned} \quad (19)$$

It gives the same expression as (19). Therefore, the minimum inductor L_{min} that limits ripple current to a value is

$$i_{\text{ripple}} = \frac{V_m M2 T_s}{4 L_{\text{min}}} \quad 2.20$$

$$L_{\text{min}} = V_m M2 T_s / 4 i_{\text{ripple}}$$

2.5 Design of output capacitor C

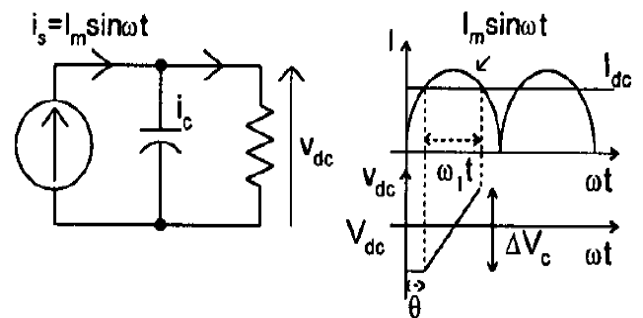


Fig. 9 Equivalent circuit in motoring mode

$$i_c(t) = i_s(t) - I_{dc}$$

$$i_s = I_m \sin \omega t \quad (21)$$

Where I_m is the peak input current, ω is the angular frequency of the ac main, and I_{dc} is the dc link current.

In steady state, the average value of is equals I_{dc} . Thus

$$I_m = \frac{\pi}{2} I_{dc} \quad (22)$$

and

$$C \frac{dV_{dc}}{dt} = i_c(t)$$

$$K_p = 0.9 T/L$$

$$C \geq \frac{I_{dc}}{\omega \Delta V_{dc, \max}} (\pi \cos \theta - \pi + 2\theta)$$

2.6 Modelling of Dc-Dc Converters $\theta = \sin^{-1} \frac{2}{\pi}$

By using the state-space averaging model of boost converter can be written as

$$A = A_{on} d + A_{off} (1-d)$$

$$B = B_{on} d + B_{off} (1-d)$$

$$\begin{bmatrix} \frac{di_L}{dt} \\ \frac{dV_c}{dt} \end{bmatrix} = \begin{bmatrix} 0 & \frac{d-1}{L} \\ \frac{1-d}{L} & -\frac{1}{RC} \end{bmatrix} \begin{bmatrix} i_L \\ V_c \end{bmatrix} + \begin{bmatrix} \frac{1}{L} \\ 0 \end{bmatrix} E$$

(23)

3. Design of PI controller

$$T_i = L/0.3$$

Where

T is time constant

L is dead time

From the response

$$\begin{matrix} T=0.0165 \text{ sec} \\ L=0.0015 \text{ sec} \end{matrix}$$

Then,

$$K_p = 0.9 * 0.0165/0.0015=10.5$$

$$T_i = 0.0015/0.3=0.005\text{sec}$$

$$\text{Transfer function} = K_p(1+1/T_iS)=10.5(1+1/.005S)$$

After tuning the K_p and T_i

Now,

$$T.F=.4(S+600)/S$$

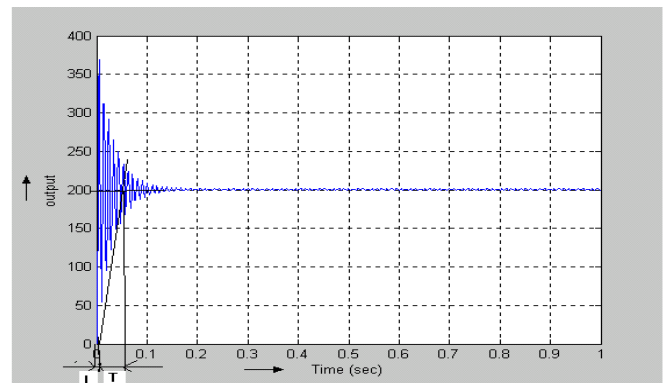


Fig. 10 PI response

3.1 Design of low pass filter

Transfer Function= $1/(1+SRC)$

Choose cut-off frequency= $f_c=79\text{Hz}$

Capacitor range from $0.1\mu\text{f}$ to $.001\mu\text{f}$

Choose capacitor= $.01\mu\text{f}$

$$f_c = \frac{1}{2\pi RC}$$

$$R = \frac{1}{2\pi * 79 * .01\mu} = 200\text{K}\Omega$$

T.F= $0.002/(s+500)$

3.2 Design of inductor average current controller

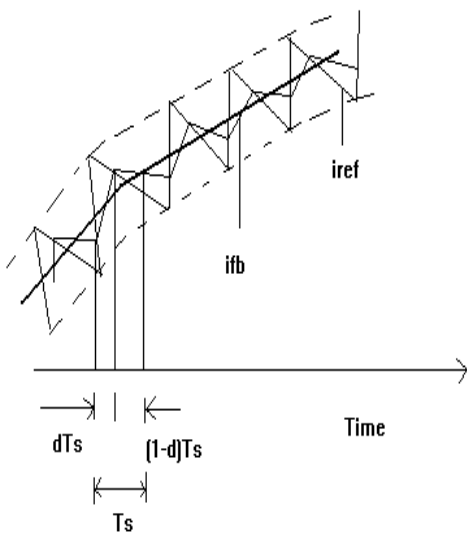


Fig.11 Waveforms of ifb and iref

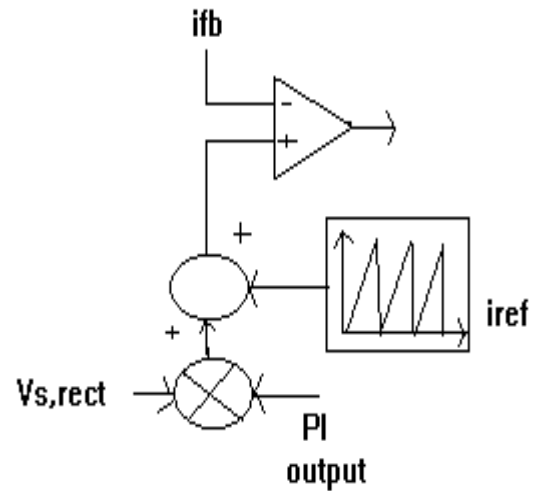


Fig.12 Inductor average current controller

In Fig.12 the PI controller output and full bridge diode rectifier output are applied to multiplier. Now, multiplier multiplies the both signal to form the modulating signal. This modulating signal and ramp function are applied to summer. It's sums the both signal to form reference current.

Then reference current is compared to feedback current to form pwm pulse to control the switch S1. The duty cycle of the switch S1 can be varied by changing the ramp function magnitude. In Fig.11 the feedback current is compared with reference sinusoidal waveform and is forced to remain between the maximum and minimum values of iref.

3.3 Synchronization and triggering circuit

Fig. 13 show Simulink diagram of synchronization circuit.

$$C \geq \frac{I_{dc}}{\omega \Delta V_{dc, \max}} (\pi \cos \theta - \pi + 2\theta) \geq \frac{2.5}{2 * \pi * 50 * 5} (\pi * \cos \theta - \pi + 2\theta) \geq 200 \mu F$$

$$\Delta V_{dc, \max} = 5V$$

$$I_s = \frac{500}{100} = 5A$$

$$\theta = \sin^{-1} \frac{2}{\pi}$$

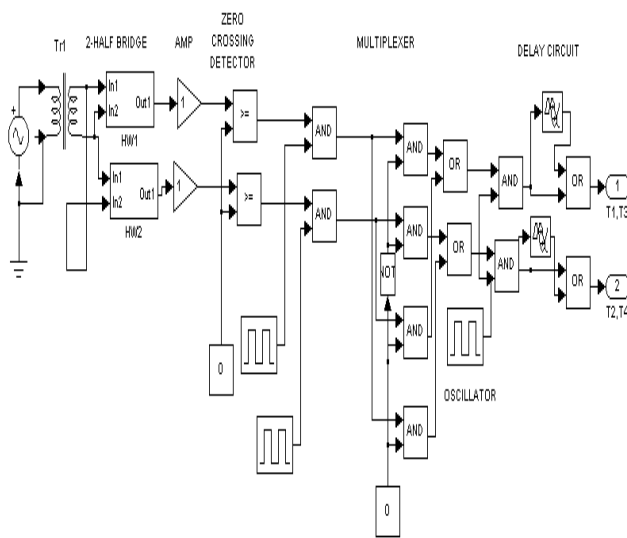


Fig. 13 Synchronization and triggering circuit

3.4 Design specification of proposed converter

$$V_s = V_m \sin \omega t = 100 * \sqrt{2} \sin 2 * \pi * 50 * t$$

$$V_m = 141V$$

$$V_s = 100V$$

$$\text{Switching frequency} = 40KHz$$

$$T_s = 25 \mu sec$$

Choose, $I_{ripple} = 10\%$ of I_s

Output voltage is assumed to be constant,

$$V_{out} = 200$$

$$M1 = M2 = M = \frac{V_{out}}{V_m} = \frac{200}{141.41} = 1.42$$

The conversion efficiency is assumed to be 100%

Input power = Output power

Load resistance

$$R = \frac{V_{out}^2}{P_o} = \frac{(200)^2}{500} = 80 \Omega$$

$$I_{ripple, \max} = 0.1 * \frac{P * 2}{V_m} = 0.1 * \frac{500 * 2}{141} = 0.714A$$

$$L_{\min} = \frac{V_m M T_s}{4 I_{ripple, \max}} = \frac{141.14 * 1.42 * 25 * 10^{-6}}{4 * .71} = 1.76mH$$

$$I_{ref} = \frac{\sqrt{2} * 2 * P}{\eta * V_{rms}} = \frac{\sqrt{2} * 2 * 500}{1 * 100} = 10A$$

Motoring mode:

$$\frac{|V_s|}{V_{out}} = 1 - d$$

$$|V_s| = \frac{2V_m}{\pi} \cos \alpha = \frac{2 * 141}{\pi} \cos 345 = 88.9V$$

$$1 - d = \frac{88.9}{200}$$

$$d = 0.5667$$

$$T_{on} = d T_s = 0.5667 * 25 * 10^{-6} = 14.16 \mu sec$$

Regenerating mode:

$$\frac{|V_s|}{V_{out}} = d$$

$$|V_s| = \frac{2V_m}{\pi} \cos\alpha = \left| \frac{2 \cdot 141}{\pi} \cos 165^\circ \right| = 88.9V$$

$$d = \frac{88.9}{200}$$

$$d = 0.4335$$

$$T_{on} = dT_s = 0.4335 \cdot 25 \cdot 10^{-6} = 10.68 \mu\text{sec}$$

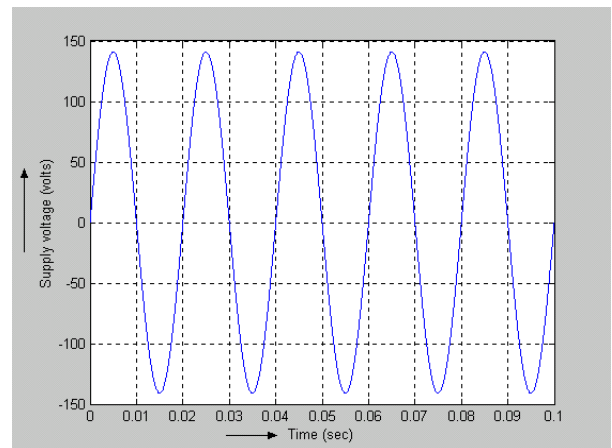


Fig. 15. Simulated supply voltage of proposed converter with controller

4. Simulation results and discussion

In this part, the simulation results for both closed loop motoring mode and regenerating mode is presented.

4.1 Motoring mode (closed loop)

Figs. 14 to 21 show the simulated responses of proposed converter during motoring mode. From these results, it is clearly found that designed converter with controller has produced unity power factor and excellent output voltage regulation.

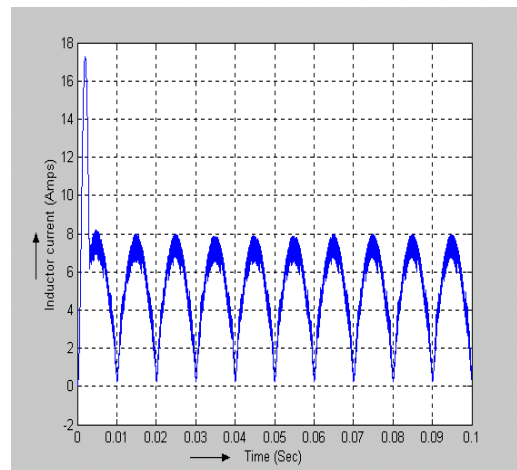


Fig.16. Simulated inductor current of proposed converter with controller

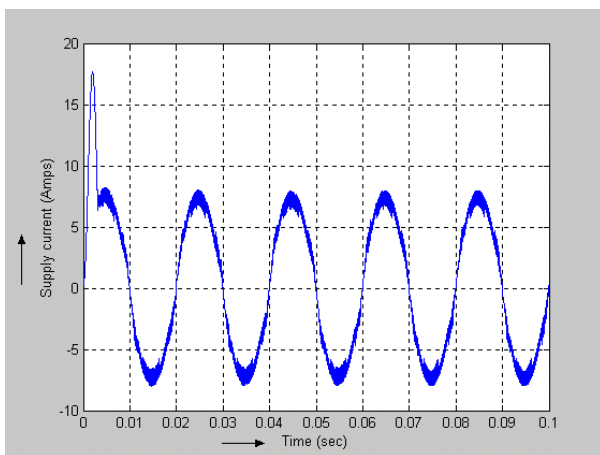


Fig. 14. Simulated supply current of proposed converter with controller

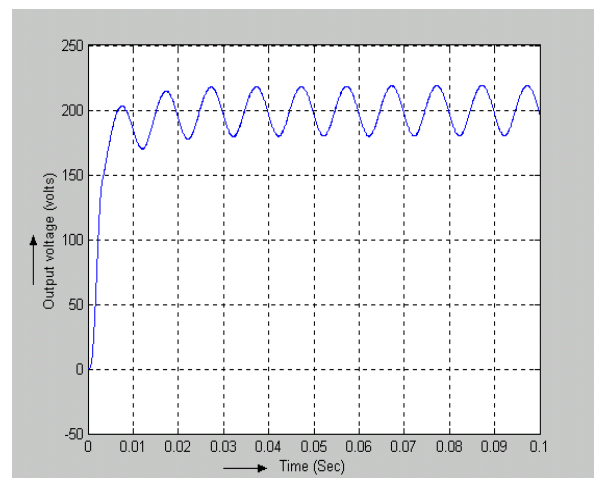


Fig. 17. Simulated output voltage of proposed converter with controller

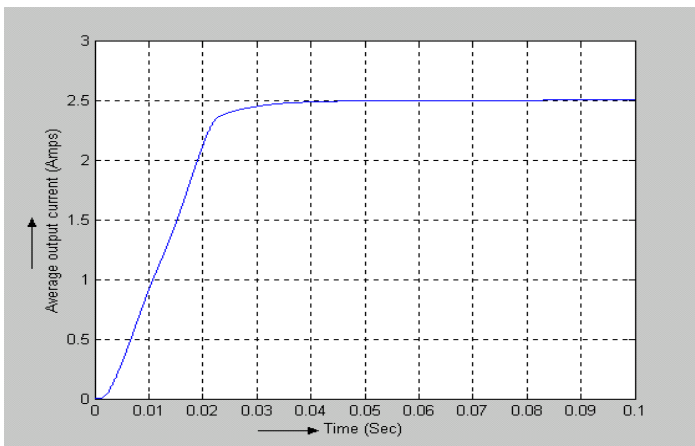
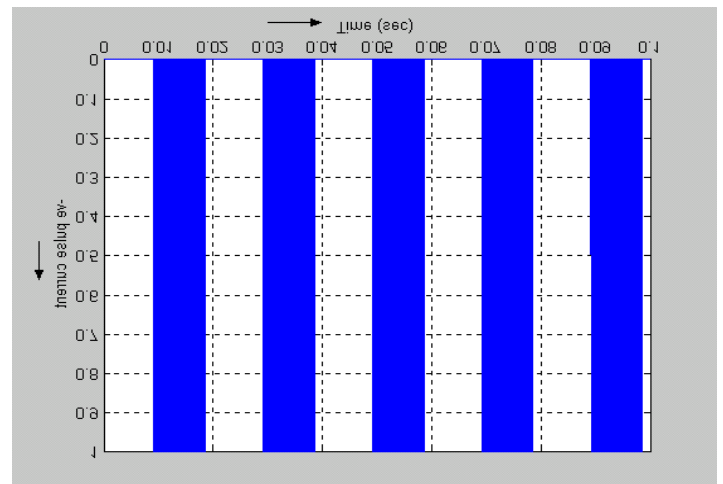


Fig. 18. Simulated average output current of proposed converter with controller



(b)

Fig. 20. (a) and (b) Simulated thyristor firing pulse of proposed converter with controller

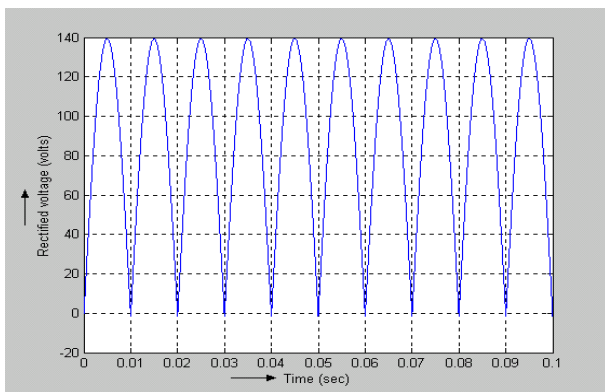


Fig. 19. Simulated thyristor rectified voltage of proposed converter with controller

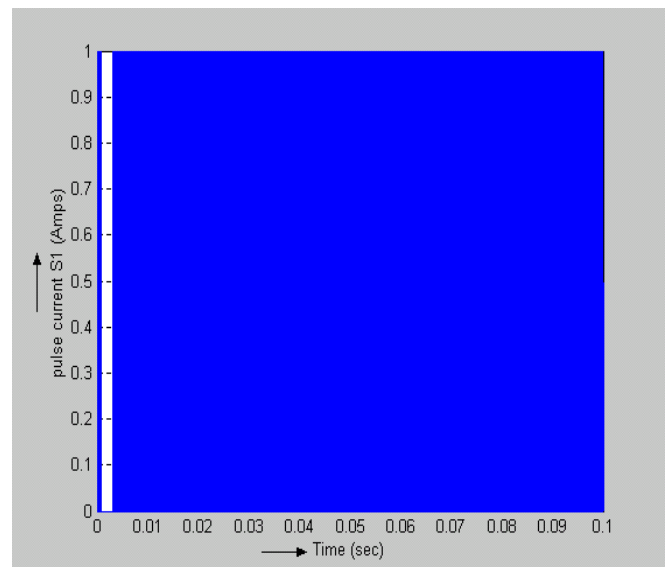
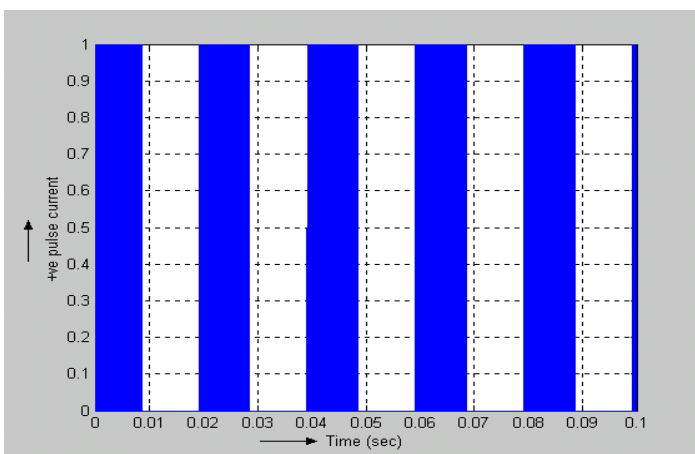


Fig. 21. Simulated PWM pulse for switch S1



(a)

4.2 Regenerating mode (closed loop)

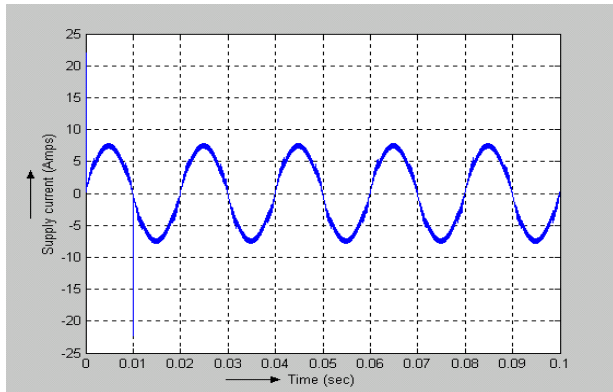


Fig.22. Simulated supply current of proposed converter with controller in regenerating mode

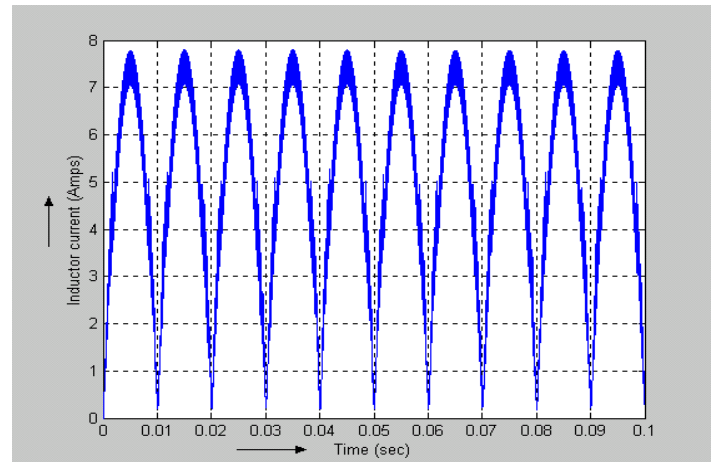


Fig. 24. Simulated inductor current of proposed converter with controller in regenerating mode.

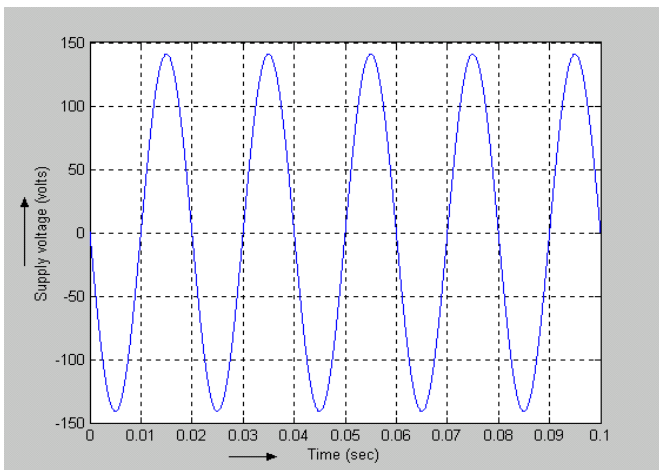


Fig. 23. Simulated source voltage of proposed converter with controller in regenerating mode.

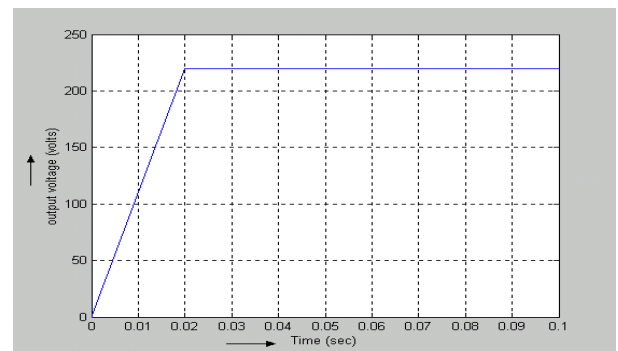


Fig. 25. Simulated average output voltage of proposed converter with controller in regenerating mode

Figs. 22 to 28 show the simulated responses of proposed converter during regenerating mode. From these results, it is clearly found that designed converter with controller has produced unity power factor and excellent output voltage regulation.

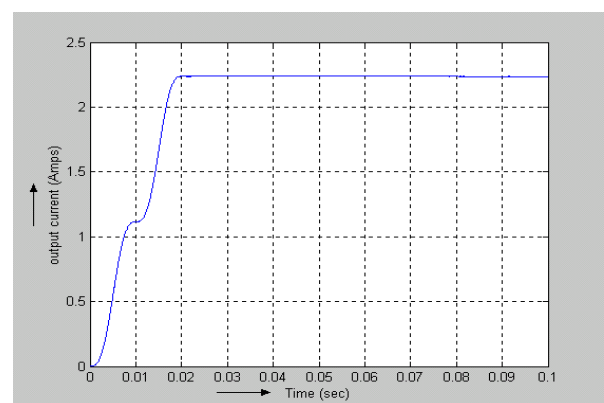


Fig. 26. Simulated average output of proposed converter with controller in regenerating mode.

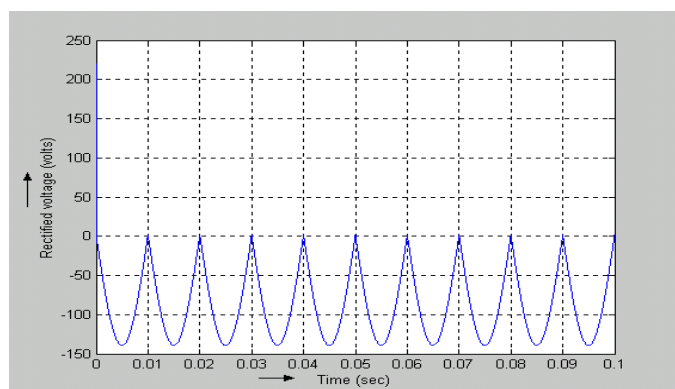


Fig. 27. Simulated rectifier output voltage of proposed converter with controller in regenerating mode.

validated through the MATLAB/Simulink. The control scheme used in this converter is simple and commonly used in current controlled power converter. The designed controller has produced excellent performance.

REFERENCES

- [1] Zhu. M., Luo.F.L., “Implementing of developed voltage lift technique on SEPIC, CUK and double-output DC–DC converters”, *IEEE Trans. Ind. Electron. Appl.*, Vol. 23, No. 25, pp. 674–681, 2007.
- [2] M. Jinno, P. Y Chen, Y. C. Lai, and K. Harada, “Investigation on the ripple voltage and the stability of synchronous rectifier buck converters with high output current and low output voltage”, *IEEE Trans. Ind. Electron.*, Vol. 57, No. 3, pp. 1008-1016, 2010.
- [3] J. A. Morales-Saldana, R. Galarza-Quirino, J. Leyva-Ramos, E. E. Carbajal-Gutierrez and M. G. Ortiz-Lopez, "Modeling and control of a cascaded boost converter with a single switch", *IECON 2006 - 32nd Annual Conference on IEEE Industrial Electronics*, pp. 591-596, 2006.
- [4] Luo, F.-L., Hong Ye, “Advanced DC/DC converters”, CRC Press. London, 2006.
- [5] F.J perez-Pinal and I. Cervantes, “Multi-objective control for cascade boost converter with single active switch”, *2009 IEEE International Electric Machines and Drives Conference*, pp. 1858-1862, 2009.
- [6] F. L. Luo, H. Ye, “Positive output cascade boost converters”, in *IEE Proceedings - Electric Power Applications*, Vol. 151, No. 5, pp. 590-606, 2004.
- [7] Davood Ghaderi, Mehmet Çelebi, “Implementation of PI controlled cascaded boost power converters in parallel connection with high efficiency”, *Journal of Electrical Systems*, Vol. 13, No.2, pp. 307-321, 2017.
- [8] Pinaa, P. Ferrãoa, J. Fournierb., B. Laca, “Small signal modeling of a DC-DC type double boost converter integrated with SEPIC converter using state space averaging approach”, *Energy Procedia*, Vol. 117, pp. 835-846, 2017.
- [9] Wan, X., Zhang, K., Ramkumar, S., Deny, J., Emayavaramban, G., Ramkumar, M. S., & Hussein,

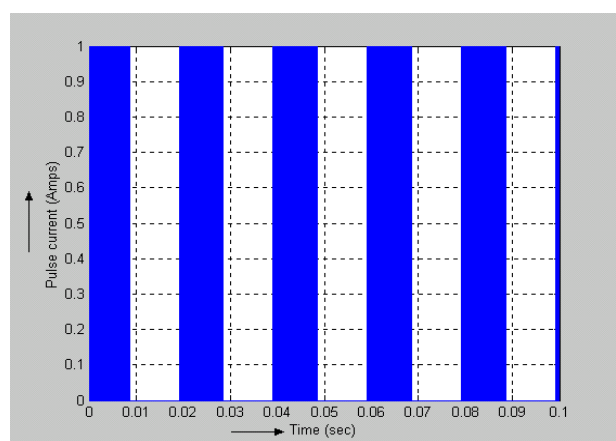
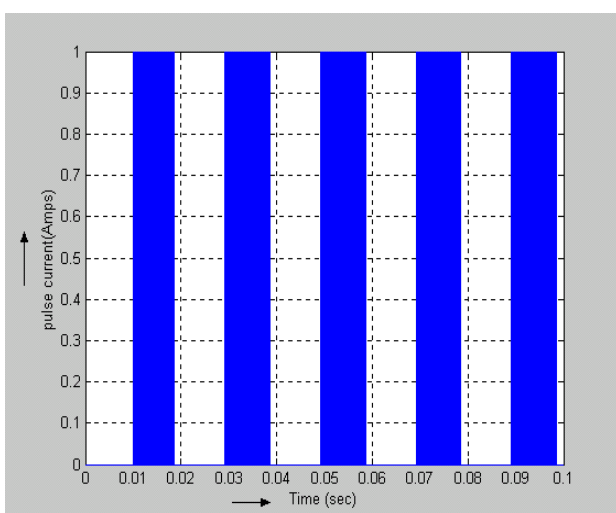


Fig. 28. Simulated thyristor firing pulse

5. Conclusions

The proposed bidirectional ac-dc power converter was studied and the designs and performance is

- A. F. (2019). A Review on Electroencephalogram Based Brain Computer Interface for Elderly Disabled. *IEEE Access*, 7, 36380-36387.
- [10] Sanjeevikumar Padmanaban, Emre Ozsoy, Viliam Fedák and Frede Blaabjerg, “Development of sliding mode controller for a modified boost Cuk converter configuration”, *Energies*, Vol.10, No.1513, 2017.
- [11] Ahmed A. A.Hafez, “Multi-level cascaded DC/DC converters for PV applications”, *Alexandria Engineering Journal*, Vol.54, No. 4, pp. 1135-1146, 2015.
- [12] Ayhan Ozdemir, Zekiye Erdem, “Double-loop PI controller design of the DC-DC boost converter with a proposed approach for calculation of the controller parameters”, *Systems and Control Engineering*, Vol. 232, No. 2, pp. 137–148, 2018.
- [13] P.Nagaveni, M.Siva RamKumar, M.Nivetha, A.Amudha, G.Emayavaramban, “Electrical Energy Audit –An Experience in a Small Scale Textile Mill” *International Journal of Innovative Technology and Exploring Engineering*, 8(10) pp 4102-4107
- [14] Balachander Kalappan, D., & Ponnusamy, V. (2013). Optimization of Cost of Energy of Real Time Renewable Energy System Feeding Commercial Load Case Study: A Textile Show Room in Coimbatore, India. *Life Science Journal*, 10(7s).
- [15] Wan, X., Zhang, K., Ramkumar, S., Deny, J., Emayavaramban, G., Ramkumar, M. S., & Hussein, A. F. (2019). A Review on Electroencephalogram Based Brain Computer Interface for Elderly Disabled. *IEEE Access*, 7, 36380-36387.
- [16] Sivaram Krishnan, M., Amudha, A., & Siva Ramkumar, M. (2018). Execution Examination Of Three Phase Ac To Three Phase Ac Matrix Converter Using Distinctive Transporter Based Exchanging Algorithms. *International journal of Pure and Applied Mathematics*, 118(11), 609-617.
- [17] Amudha, D. A., Ramkumar, M. S., & Krishnan, M. S. DESIGN AND SIMULATION OF ZETA CONVERTER WITH ZVZCS SWITCHING TECHNIQUE. *Journal of Engineering and Applied Sciences*, 14(9), 2764-2774.
- [18] Ali, M. V. M., Babar, M., Nguyen, P. H., & Cobben, J. F. G. (2017). Overlaying control mechanism for solar PV inverters in the LV distribution network. *Electric Power Systems Research*, 145, 264-274.
- [19] Mawarni, D. E., Ali, M. V. M., Nguyen, P. H., Kling, W. L., & Jerele, M. (2015, September). A case study of using OLTC to mitigate overvoltage in a rural european low voltage network. In *2015 50th International Universities Power Engineering Conference (UPEC)* (pp. 1-5). IEEE.
- [20] Ali, M. V. M., Nguyen, P. H., & Cobben, J. F. G. (2016, October). Coordinated control to mitigate over voltage and under voltage in LV networks. In *2016 IEEE PES Innovative Smart Grid Technologies Conference Europe (ISGT-Europe)* (pp. 1-5). IEEE.
- [21] Ali, M. V. M., Paterakis, N. G., Nguyen, P. H., & Cobben, J. F. G. (2017, June). A LV network overvoltage mitigation strategy based on epsilon-decomposition. In *2017 IEEE Manchester PowerTech* (pp. 1-6). IEEE.
- [22] Ali, M. V. M., Nguyen, P. H., & Cobben, J. F. G. (2016, December). Internet of things in LV grids: Framework and experiments. In *2016 Saudi Arabia Smart Grid (SASG)* (pp. 1-5). IEEE.
- [23] Viyathukattuva, Mansoor & Amudha, Alagarsamy & Ramkumar, M.Siva & Gopalakrishnan, G Emayavarmban. (2019). Relation between Solar PV Power Generation, Inverter Rating and THD. *International Journal of Advanced Manufacturing Technology*. 9. 4570-4575.
- [24] T. Kalimuthu, M. Siva Ramkumar, Dr.A. Amudha, Dr.K. Balachander and M. Sivaram Krishnan “A High Gain Input-Parallel Output-Series DC/DC Converter with Dual Coupled-Inductors” *Journal of Advanced Research in Dynamical and Control Systems*, (12), pp 818-824
- [25] S. Tamil Selvan, M. Siva Ramkumar, Dr.A. Amudha, Dr.K. Balachander and D. Kavitha “A DC-DC Converter in Hybrid Symmetrical Voltage Multiplier Concept” *Journal of Advanced Research in Dynamical and Control Systems*, (12), pp. 825-830
- [26] M. Jayaprakash, D. Kavitha, M. Siva Ramkumar, Dr.K. Balacahnder and M. Sivaram Krishnan, “Achieving Efficient and Secure Data Acquisition

- for Cloud-Supported Internet of Things in Grid Connected Solar, Wind and Battery Systems” Journal of Advanced Research in Dynamical and Control Systems, (12), pp 966-981 .
- [27] D. Kavitha, M. Siranjeevi, Dr.K. Balachander, M. Siva Ramkumar and M. Sivaram Krishnan “Non Isolated Interleaved Cuk Converter for High Voltage Gain Applications” Journal of Advanced Research in Dynamical and Control Systems, 10(5), pp 1256-1261
- [28] S.Vivekanandan, M. Siva Ramkumar, Dr.A.Amudha, M. Sivaram Krishan, D. Kavitha “Design and Implementation of Series Z-Source Matrix Converters” Journal of Advanced Research in Dynamical and Control Systems, 10(5) , pp 1095-1102
- [29] N. Eswaramoorthy, Dr.M. Siva Ramkumar, G. Emayavaramban, A. Amudha, S. Divyapriya, M. Sivaram Krishnan, D. Kavitha “A Control Strategy for A Variable Speed Wind Turbine with A Permanent Magnet Synchronous Generator Using Matrix Converter with SVPWM” International Journal of Recent Technology and Engineering, 8(1S4) pp 178-186
- [30] P. Jeyalakshmi, Dr.M. Siva Ramkumar, IR.V. Mansoor, A. Amudha, G. Emayavaramban, D. Kavitha, M. Sivaram Krishnan, “Application of Frequency based Matrix Converter in Wind Energy Conversion System Employing Synchronous Generator Using SVPWM Method” International Journal of Recent Technology and Engineering, 8(1S4) pp 187-195
- [31] Charles Stephen, .A. Amudha, K. Balachander, .Dr.M. Siva Ramkumar, G. Emayavaramban, IR.V. Manoor, “Direct Torque Control of Induction Motor Using SVM Techniques” International Journal of Recent Technology and Engineering, 8(1S5) pp 196-202
- [32] N. Saravanakumar, A. Amudha, G. Emayavaramban, Dr.M. Siva Ramkumar, S. Divyapriya, “Stability Analysis of Grid Integration of Photovoltaic Systems Using Partial Power Converters” International Journal of Recent Technology and Engineering, 8(1S5) pp 203-210
- [33] S.Divyapriya, K.T.Chandrasekaran, A.Amudha, Dr.M.Siva Ramkumar, G.Emayavaramban, “Low Cost Residential Micro Grid System based Home to Grid Backup Power Management” International Journal of Recent Technology and Engineering, 8(1S5) pp 303-307
- [34] N. Thiyaagarajan, Dr.M. Siva Ramkumar, A. Amudha, G. Emayavaramban, M. Sivaram Krishnan, D. Kavitha, “SVPWM based Control of SCIG-Matrix Converter for Wind Energy Power Conversion System” International Journal of Recent Technology and Engineering, 8(1S5) pp 211-218
- [35] N. Seethalakshmi, A. Amudha, S. Divyapriya, G. Emayavaramban, Dr.M. Siva Ramkumar, IR.V. Mohamed Mansoo, “Voltage Frequency Controller with Hybrid Energy Storage System for PMSG Based Wind Energy Conversion System” International Journal of Recent Technology and Engineering, 8(1S5) pp 219-229
- [36] G. Suresh, A.Amudha, Dr.M. Siva Ramkumar,G. Emayavaramban, IR.V.Manoor, “Bidding Strategy of Electricity Market Considering Network Constraint in New Electricity Improvement Environment” International Journal of Recent Technology and Engineering, 8(1S5) pp 230-234
- [37] G. Krishnan, M. Siva Ramkumar, A. Amudha, G. Emayavaramban,S. Divyapriya, D. Kavitha, M. Sivaram Krishnan, “Control of A Doubly Fed Induction Generator for Wind Energy Conversion System Using Matrix Converter with SVPWM Technique” International Journal of Recent Technology and Engineering, 8(1S5) pp 235-243
- [38] S. Viswalingam, G. Emayavaramban, Dr.M. Siva Ramkumar, A. Amudha, K. Balachander, S. Divyapriya, IR.V. Mohamed Mansoor “Performance Analysis of a Grid Connected PV-Wind with Super Capacitor Hybrid Energy Generation & Storage System” International Journal of Recent Technology and Engineering, 8(1S5) pp 658-666
- [39] N.Pandiarajan, G.Emayavaramban, A.Amudha, Dr.M.Siva Ramkumar, IR.V.Mohamed Mansoor, K.Balachander, S.Divyapriya, M..Sivaram Krishnan, “Design and Electric Spring for Power Quality Improvement in PV-Based Dc Grid” International Journal of Recent Technology and Engineering, 8(1S5) pp 242-245
- [40] V.Jayaprakash, S.Divyapriya, A.Amudha, G.Emayavaramban,Dr.M.Siva Ramkumar, “Nano -

Grid Smart Home With Plug-in Electric Vehicle using a Hybrid Solar-Battery Power Source” International Journal of Recent Technology and Engineering, 8(1S5) pp 246-248

- [41] K.T.Chandrasekaran, S.Divyapriya, A.amudha, Dr.M.Siva Ramkumar, G.Emayavaramban, “Modeling and Control of Micro Grid Based Low Price Residential Home to Grid Power Management System” International Journal of Recent Technology and Engineering, 8(1S5) pp 261-265.